Numerical Analysis and Prediction of Flow Field in Horizontal Turbine

Shengyang Peng[1]，Guofeng Dong*[2]，Zhenggui Li*[1]，Shiyang Pan[1]，
Liang Zheng[2]，Biao Ma[2]

1.Key Laboratory of Fluid and Power Machinery,Ministry of Education,
Xihua University,a541792386@qq.com,Chengdu,China
2.International Center on Small Hydro Power,Hangzhou ,China
E-mail (corresponding author):lzhgui@126.com

Abstract

In order to study the interaction of vortex structure,vortex evolution and vortex in a tubular turbine,the regularized helicity, Q-criterion and BVF diagnosis based on RNG $k-\varepsilon$ turbulence model and vortex dynamics diagnosis method are applied to a tubular turbine under certain working conditions.The vortex motion was numerically studied. Turbulent vortex movements dominate the turbine operation. Compared with the cloud diagrams of pressure,streamline and velocity observed by the numerical methods, the vortex dynamics diagnosis can accurately capture the vortex structure,the distribution of vortexes and the intensity variation of the turbine runner and the draft tube. By applying the vortex dynamics criterion,it is found that there is a vortex in the direction of rotation and the flow direction of the water flowing near the water inlet edge and the hub of the front runner of the turbine runner. At the back of the hub,there is a vortex with a direction of rotation and a direction of flow opposite the inlet. The application of vortex dynamics diagnosis found that the flow separation zone and the BVF peak zone on the turbine runner blades are more accurate than the traditional analysis methods.The application of vortex dynamics diagnosis on the tubular turbine provides a new perspective for turbine runner optimization and a new idea for changing the flow in the digital turbine.
Key Words： Bulb tubular turbine Numerical simulation   Vorticity Vortex

1. Introduction

The tubular turbine is suitable for low-head, high-flow hydropower units and is the main unit for generating electricity in low-head areas[1].With the development of computer technology and computational fluid dynamics,numerical simulation has become an important means in the field of hydraulic machinery design and research.The traditional analysis method is to judge the flow performance of the flow component from the macroscopic point by the pressure distribution or the velocity vector in the calculation result,but the parameters such as pressure and velocity in the flow field are continuously changed.Therefore,the flow state cannot be revealed.The internal causes of deterioration and instability of the unit.The results of this analysis are not comprehensive,and the design optimization is not perfect[2].

The fluid in the turbine is vortex-moving,and the flow pattern is very complicated and unsteady.There are obvious vortex flow and flow separation in the turbine runner,which is directly related to the efficiency and stability of the turbine.The vortex motion and the separation flow in the turbine are common flow phenomena.A vortex is a group of fluid micelles that rotate around a common center.It is a finite volume of swirling fluid bounded by a non-rotating fluid or object plane.It has the participation of vortex in most fluid motions[3].Therefore, the precise acquisition of the vortex motion structure can intuitively reflect the flow field changes.

Vortex dynamics[4] is an important branch of computational fluid dynamics, and its development has been relatively mature.In fluid mechanics,vortex has not been accurately defined mathematically to date.Although in some simple flows,one can determine the existence of vortex by intuition and image, in complex flows such as three-dimensional viscous,especially turbulent flow, the interaction of vortex,vortex evolution and vortex can be demonstrated from experimental or direct numerical simulations.It is very necessary to gradually form a vortex criterion method that does not depend on coordinate selection and rotation changes in a large number of experimental and numerical computational complex flows: regularized helicity,maximum vorticity method, Q-criterion, Δ-criterion, λ_2-criterion,helicity method,vortex current parameter method,etc. [5].

Li Fengchao et al.[2] used BVF diagnosis to optimize the turbine blades,and after optimization,the turbine runner efficiency was improved.Wu Xiaojing et al.[6] used the vortex dynamics theory to optimize the Francis turbine runner, and improved the performance of the runner's overcurrent capability,functional force and efficiency.Zhang Liang et al.[7] carried out vortex dynamic analysis on the internal flow field of the runner,and found that traditional analysis methods such as pressure and streamline are not as clear and accurate as BVF convection field analysis.Yang Lin et al.[8-9] used the local vortex dynamics diagnostic method to diagnose the bidirectional three-dimensional flow field in the designed

reversible wheel,which improved the efficiency and cavitation performance of the runner.Zhao Binjuan et al.[10] introduced boundary vorticity dynamics theory to optimize the dual-channel pump impeller.After optimization, the impeller stress condition was improved,and the hydraulic performance such as lift and efficiency were significantly improved.Zhao Youfei[11] used boundary vorticity dynamics and artificial neural network algorithm to optimize the centrifugal pump impeller,and found a new method to optimize the impeller in the crossover algorithm.Wang Yang et al.[12] introduced the Q-criterion to analyze the hydraulic performance of multistage centrifugal pumps and analyzed the vorticity to find out the cause of the sharp drop in the lift.

There are few studies on the overall vortex dynamics of the Tubular Turbine. Therefore,for the tubular turbine,the vortex dynamics diagnosis method for vortex and vorticity field is used to analyze the vortex structure of the turbine runner and the draft tube and other overcurrent components.The diagnosis of the rotor blade is carried out in combination with the BVF distribution,which provides a direct and reasonable diagnosis basis for the optimized design of the tubular turbine flow component.

2. Computational simulation

2.1 Computational model

The tubular turbine studied in this paper originates from an adjustable riverbed power station in the upper reaches of the Yellow River.The fluid domain model is shown in Fig.1.It includes the inlet section,the bulb body,the movable guide vane,the runner and the draft tube.The operating conditions are the active vane opening degree of 59.96 °and the blade opening degree of 31 °.The flow rate of this calculation condition is 320 m³/s.
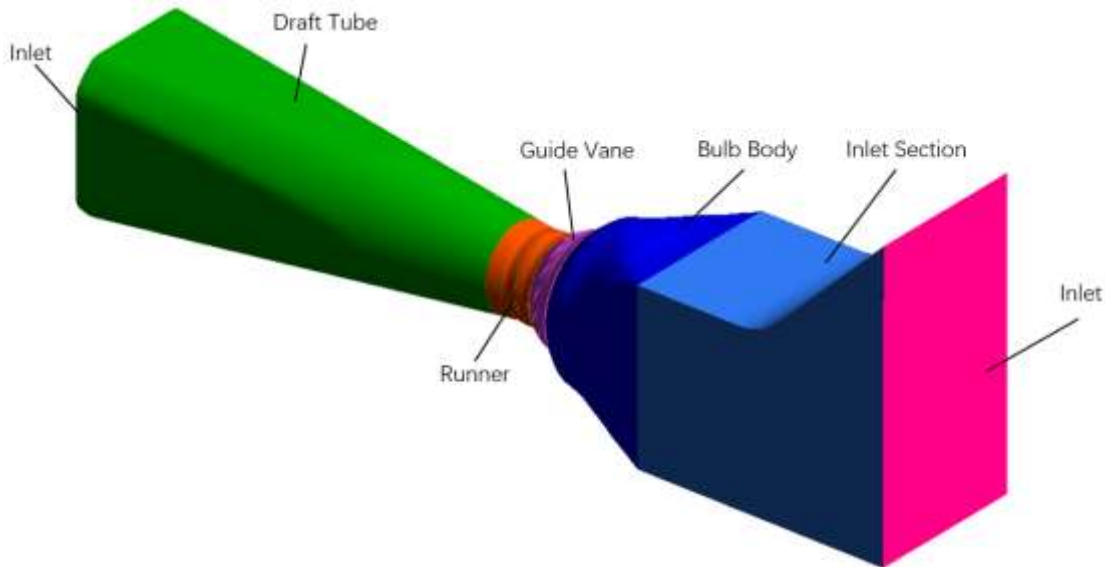
Figure 1: Computational model of tubular turbine fluid domain

2.2 Tubulence model

The selection of the turbulence model has a great influence on the accuracy of the solution.Therefore,the RNG $k-\varepsilon$ model is used.This model is derived from the mathematical method of the instantaneous Navier-Stokes equations using the renormalization group.The constants in the model are different from the standard $k-\varepsilon$ model, and new functions or terms appear in the equation.The turbulent kinetic energy and dissipation rate equations have a similar form to the standard $k-\varepsilon$ model[13]: the only difference is the c_1^* in the ε equation, which adds an item to the ε equation, reflecting the mainstream time-average strain rate E_{ij}, improving the accuracy.Taking into account the turbulent vortex, the accuracy in this respect is improved.Turbulent energy k and turbulent dissipation rate ε constraint equation:

$$\rho\frac{\mathrm{d}k}{\mathrm{d}t} = \frac{\partial}{\partial x_i}\left[\left(\alpha_k\mu_{eff}\right)\frac{\partial k}{\partial x_i}\right] + G_k + G_b - \rho\varepsilon - Y_M \qquad (1)$$

$$\rho\frac{\mathrm{d}\varepsilon}{\mathrm{d}t} = \frac{\partial}{\partial x_i}\left[\left(\alpha_\varepsilon\mu_{eff}\right)\frac{\partial\varepsilon}{\partial x_i}\right] + C_{1\varepsilon}\frac{\varepsilon}{k}\left(G_k + C_{3\varepsilon}G_b\right) - C_{2\varepsilon}\rho\frac{\varepsilon^2}{k} - R \qquad (2)$$

Where G_k represents the generation of turbulent energy due to the average velocity gradient, G_k represents the generation of turbulent energy due to buoyancy effects, and Y_M represents the effect of compressible turbulent pulsation expansion on the total dissipation rate, which is the same as in the standard $k-\varepsilon$ model. ∂_ε and ∂_k are the reciprocal of the effective flow Prandtl number of the kinetic energy k and the dissipation rate ε ,respectively.The turbulent viscosity

parameter is calculated as $d\left(\dfrac{\rho^2 k}{\sqrt{\varepsilon\mu}}\right)=1.72\dfrac{\tilde{v}}{\sqrt{\tilde{v}^3-1-Cv}}d\tilde{v}$, $\tilde{v}=\mu_{eff}/\mu$ and $C_v\approx100$. For high Reynolds numbers, the above

equation gives: $\mu_t=\rho C_\mu\dfrac{k^2}{\varepsilon}$, $C_\mu=0.0845$.

2.3 Meshing and boundary condition selection

The division of the grid has a great impact on the later computation efficiency and results.In order to improve the calculation accuracy,the inlet section, the bulb body and the draft tube fluid domain are structured grids, the number of grids is 65588, 30240, 162355,respectively.The guide vane and runner fluid domains are unstructured grids.The quantities are 5,528,362 and 30,912,201 respectively.After grid-independence verification,the total number of grid cells is finally determined to be 8877746,in which the number of nodes is 1937620,and the fluid domain grid is shown in Fig.2.

Table 1: Grid layout of turbine components

	Inlet Section	Bulb Body	Guide Vanes	Runners	Draft Tube
Grid	65588	30240	5528362	3091201	162355
Grid Node	69260	34188	1071163	594621	168388
Grid Type	Hexahedron	Hexahedron	Tetrahedron	Tetrahedron	Tetrahedron
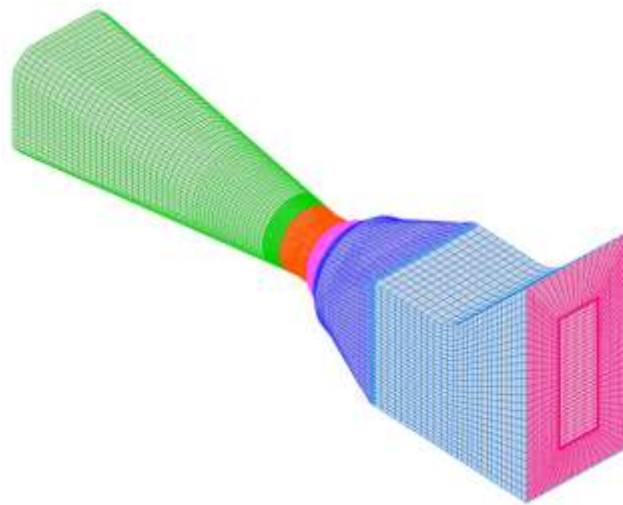
Figure 2: Tubular Turbine Fluid Domain Grid

In the computational simulation,the medium is clean water, the inlet boundary condition is one atmospheric pressure (1 atm).The inlet boundary condition selects mass flow.The exit boundary condition selects Opening as the export condition.The solid wall condition adopts no slip wall.The runner、 the vane and draft tube interaction surface adopts the Frozen Rotor method.Set the Physical Timescale to 0.00489 s.The calculated convergence accuracy is 10^{-5} .

3. Numerical Ananlysis

3.1 Traditional diagnostic analysis

The traditional diagnosis is to describe and analyze the flow field changes through the cloud maps such as pressure,velocity and velocity vector in the computational simulation post-processing, qualitative analysis of the flow field, and observation of the flow of the turbine runner and the draft tube.Fig.3(a) and (b) is the pressure cloud diagram of the front and back of the runner under the condition of $0.8Q_d$.It can be seen from the figure that as the radius increases,the pressure gradient of the runner does not change much, and the pressure of the front is larger than back.The pressure of inlet side is slightly higher than outlet,but there is no peak concentration area or obvious irregular area on the whole blade.Figure.3(c) is the pressure distribution diagram of the draft tube,the overall pressure is still very uniform,but it is seen that there is a negative value region, and the pressure value ranges from $-4.875*10^4$ Pa to $1.552*10^3$ Pa.Fig.3(d) shows the pressure distribution of the cross section of the draft tube Z=0.The pressure is also uniformly distributed,and the change is not large,and the area where the flow is unstable is not seen.

（a）Leaf front pressure distribution　（b）Pressure distribution on the back of the blade

（c）Draft tube pressure distribution　（d）Draft tube Z=0 section pressure distribution
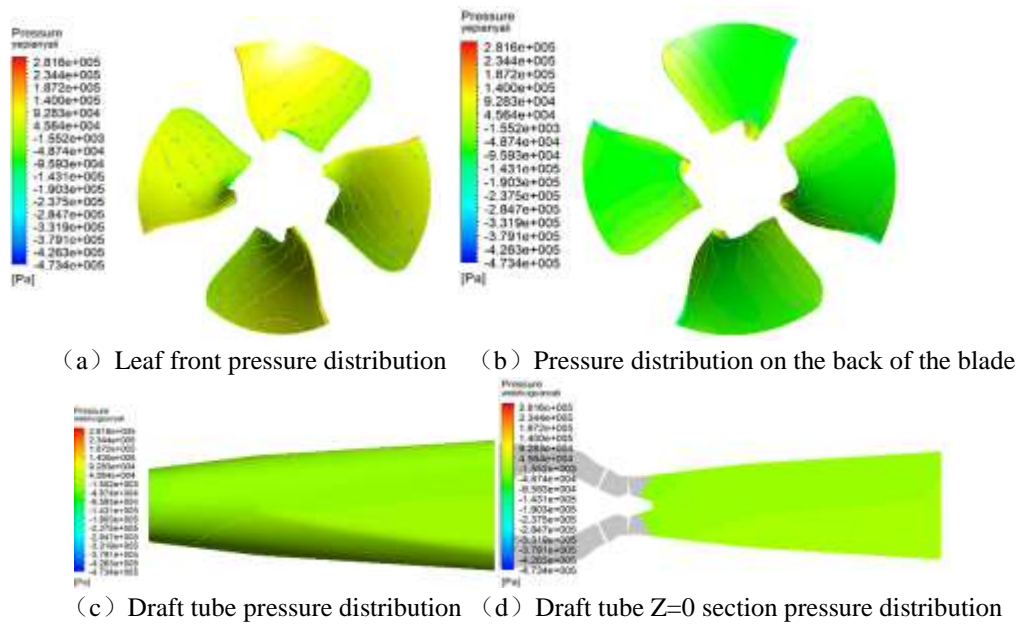
Figure 3: Pressure cloud map under $0.8Q_d$ condition

Fig.4(a) and (b) show the velocity streamline distribution on the surface of the runner blade.The streamline is evenly distributed.The velocity increases gradually along the direction of the radius increase,and the difference between the front and back velocity is small.Fig.4(c) shows the streamline distribution of the draft tube Z=0 section velocity,and the change of the velocity is small. It can be seen that there is a obvious vortex in the upper part of the outlet of the draft tube under this condition,and the flow line near the wall of the draft tube is visible.The flow line in the middle of the draft tube changes greatly,and there is a tendency to form vortex.

（a）Streamline distribution on the front of the blade （b）Streamline distribution on the back of the blade

（c）Streamline distribution of Z=0 section
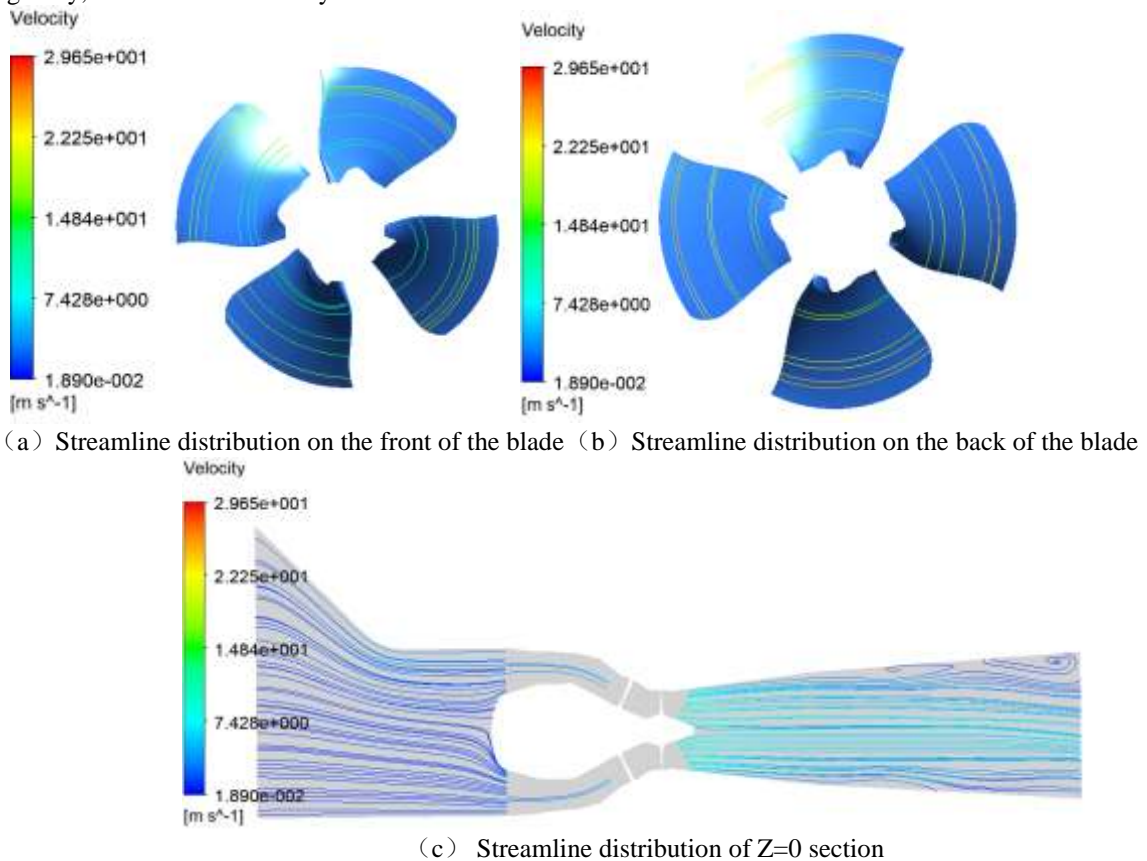
Figure 4: Streamline distribution under $0.8Q_d$ conditions

3.2 Diagnosis of vortex dynamics

The vortex is a unique form of fluid motion.The vortex includes the vorticity field and the vortex.The vorticity field refers to the spatial distribution of the vorticity.The vortex is the concentrated vortex. The vortex is a basic structure of turbulence.The source of vorticity is the existence of velocity gradient in the flow field,which is a kinematic physical quantity describing the motion of the vortex.The vorticity field will evolve into a vortex of discrete vorticity

accumulation in the fluid motion[3]. In viscous fluid mechanics,the vortex is one of the main causes of the energy loss of the liquid flow.To study the viscous flow in the turbine is inseparable to study the motion of the vortex. For the turbine, understanding the location and mechanism of the vortex motion can fundamentally control the flow separation and better optimize the structure.

3.2.1 ω - criterion

The physical quantity characterizing the angular velocity of the fluid element is called the vorticity.The place where the vorticity is extremely large is the center of the vortex.The vorticity can be understood as double the angular velocity at which the fluid micelle rotates rigidly around its center, resulting from the existence of a velocity gradient in the flow field[3].That is the rotation of the velocity field:

$$\omega = \nabla \times V \qquad (3)$$

Where: V - the velocity vector of the fluid particle; ω - the vorticity of the fluid particle.

（a）Distribution map of blade vorticity　　（b）Enlargement of blade edge vorticity
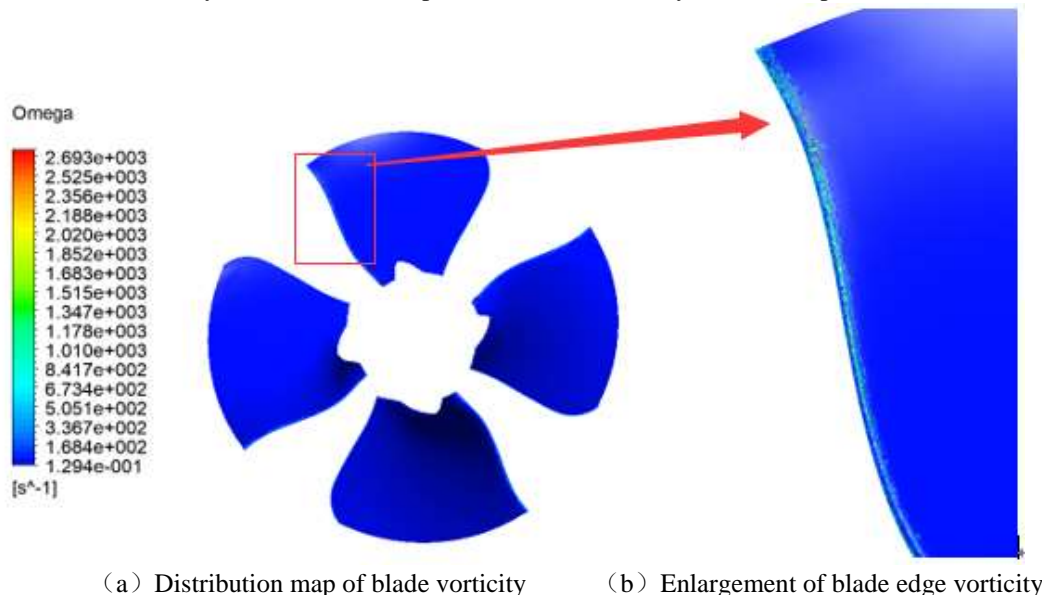
Figure 5: Vorticity cloud map of blade

It can be seen from Fig.5 that the vorticity value at the water inlet edge position is the largest, and the maximum at the rim as the radius increases, but the overall value is small.The vorticity value is $1.294*10^{-1}$-3.367 between $\times 10^2$ s^{-1}, the motion state of the vortex cannot be effectively captured. Therefore,it is impossible to judge the vortex structure and the vortex feature near the runner blade by using the vorticity modulus value.Because the vorticity value is not equal to the existence of vortices and it does not have generalized Galilean invariance[14].

3.2.2 Regularized helicity analysis

Helicity[15] is an important physical quantity that measures the topology of turbulent vorticity fields.The helicity of fluid motion in a three-dimensional flow field is defined as:

$$H(t) = \int_V V \cdot \omega \mathrm{d}V \qquad (4)$$

The integrand is called the helicity density.

The regularized helicity judges the vortex core according to the angle between the velocity vector and the vorticity.This method can capture the position of the vortex core,which is defined as the product of the dot product of velocity and vorticity divided by the modulus of the velocity and the modulus of the vorticity.Function as following:

$$H_n = \frac{V \cdot \omega}{|V| \cdot |\omega|} \qquad (5)$$

In the flow field region, it is a scalar field defined except for the special point where the velocity vector V and the vorticity vector ω are zero,and its value is in the interval [-1, 1].In the vortex core region,the velocity vector direction is nearly parallel to the vorticity vector direction, and the regularized helicity H_n tends to ± 1.The sign of the regularized helicity H_n indicates the direction of the vortex rotation, with the flow direction being the positive direction, H_n being positive,and the vortex rotating direction being counterclockwise. H_n being negative and the vortex rotating direction being clockwise[16].

Fig.6 is a regularized helicity distribution of the runner blades.It can be seen from the figure that the spiralness distribution of each blade on the front side of the blade is basically the same.On the front side,the blade inlet edge and the hub are close to the water outlet edge,and there is a vortex with the same direction of rotation and the flow direction of the water flow, H_n is in [-1, 0].The rest of the region has a vortex with the opposite direction of rotation and the flow direction of the water flow, H_n is in [0,1].On the back side,the hub has a vortex whose rotation direction and flow

direction are opposite to each other near the inlet water,and the other region has a vortex whose rotation direction and flow direction are opposite.
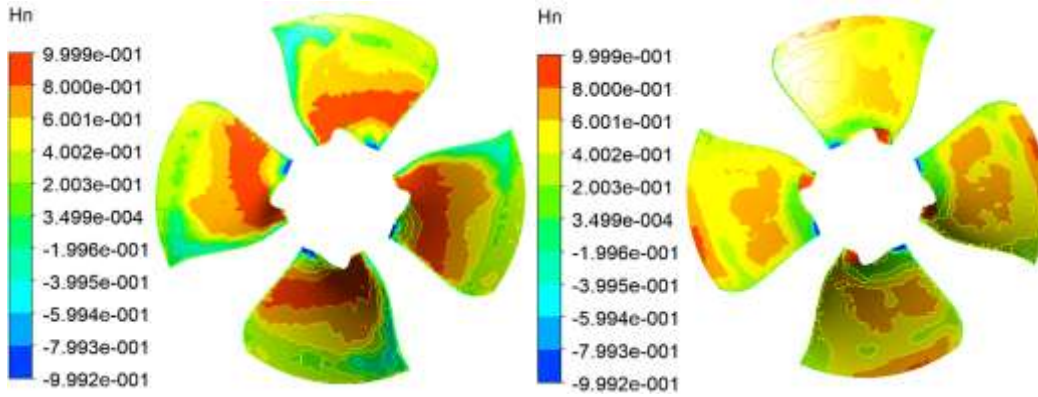
Figure 6: Regularized helicity distribution on the front and back of the runner blade
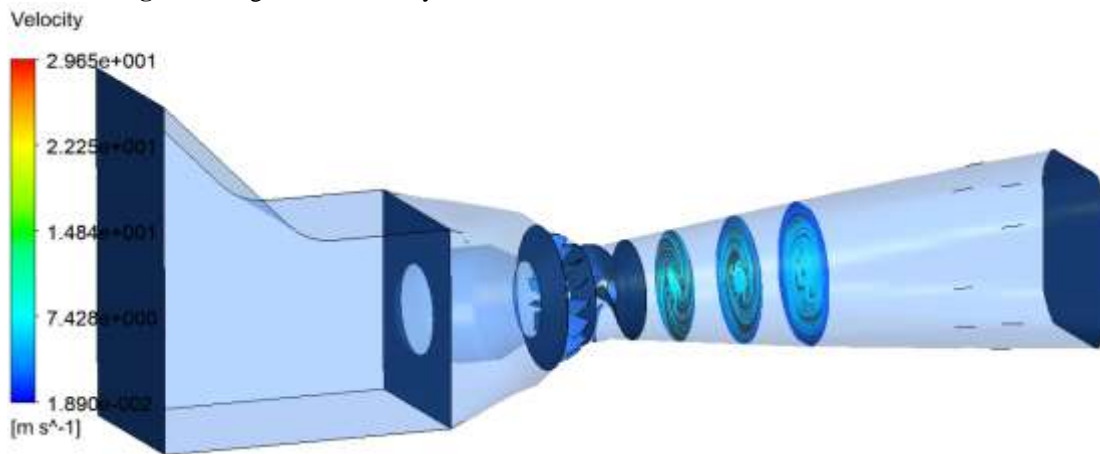
Figure 7: Three section streamlines of the draft tube
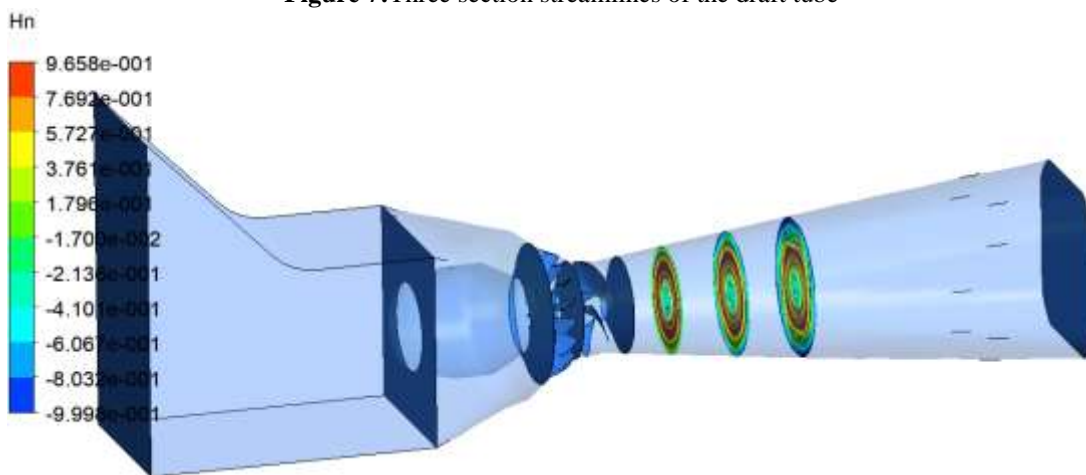
Figure 8: Three section regularized helicity distribution of draft tube

Plane3　　　　　　Plane4　　　　plane5

Plane3   Plane4   Plane5
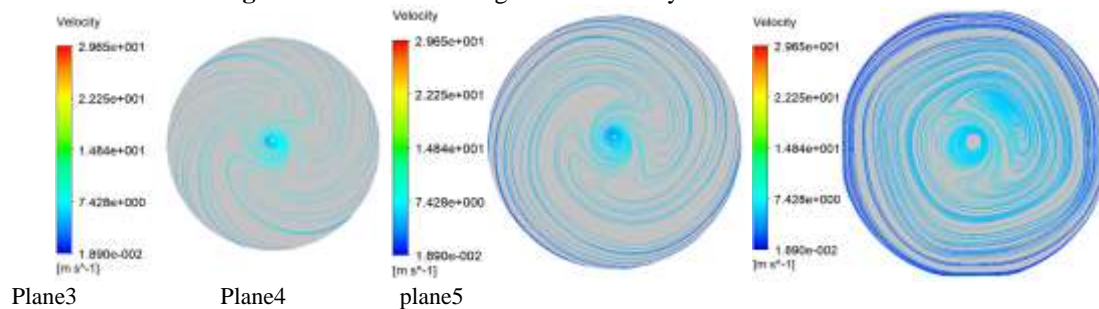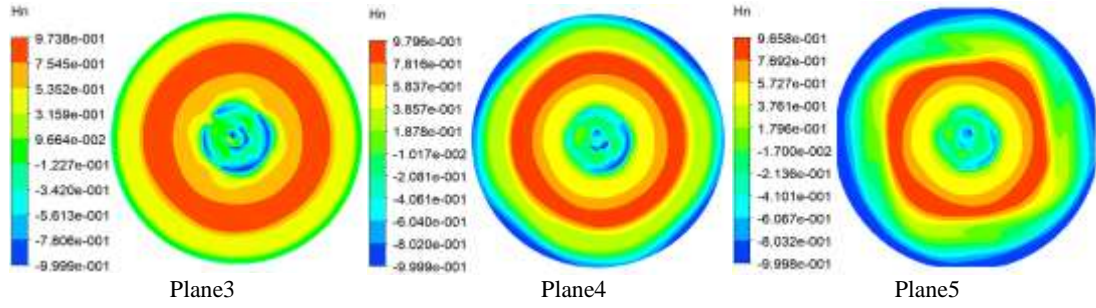
Figure 9: A enlargement of the streamline and regularized helicity of the three sections of the draft tube

Fig.9 is an enlarged view of the flow lines and regularized helicity of the three sections.It can be seen from the flow chart that there is a vortex at the center of the section, that is,in the middle of the draft tube,and Plane5 can see that there are two vortexes.From the regularized helicity diagram,it can be found that there are vortexes at the center of the three sections,and that the direction of rotation is a clockwise vortex.The vortex of the draft tube near the wall is in the same direction as the vortex of the center,and the direction of rotation between the center and the wall is opposite to the wall and the center.It can be seen that the vortex of the regularized helicity is more accurate and intuitive than the streamline,and the distribution area is also generally known.

3.2.3 Q- criterion

From the second-order tensor characteristics,the characteristic equation of the local velocity gradient tensor ∇V of the incompressible flow can be written as [3]:

$$\lambda^3 + Q\lambda - R = 0 \qquad (6)$$

If λ_1, λ_2 ,and λ_3 are its three roots,there are three independent invariants between them:

$$P = \lambda_1 + \lambda_2 + \lambda_3 = \text{div} V = 0 \qquad (7)$$

$$Q = -\frac{1}{2}\left(e_{ij}e_{ji} + \Omega_{ij}\Omega_{ji}\right) = \frac{1}{2}\left(\Omega_{ij}\Omega_{ij} - e_{ij}e_{ji}\right) = \frac{1}{2}\left(\|\Omega\|^2 - \|E\|^2\right) \qquad (8)$$

$$R = \lambda_1\lambda_2\lambda_3 = \frac{1}{3}\left(e_{ij}e_{jk}e_{ki} + 3\Omega_{ij}\Omega_{jk}e_{ki}\right) \qquad (9)$$

e_{ij} and Ω_{ij} are the strain rate tensor and vorticity tensor,respectively, $\Omega_{ij} = -\Omega_{ji}$, $\|\Omega\|^2 = \Omega_{ij}\Omega_{ji} = \frac{1}{2}|\omega|^2$.

Hunt et al.(1988) proposed that the region of $Q > 0$ be defined as a vortex, this means that $\|\Omega\|^2 > \|E\|^2$, the rotation of the fluid (the magnitude of the vorticity) in the region of the vortex dominates the magnitude of the strain rate,which is said to be the Q-criterion.

（a）

（b）
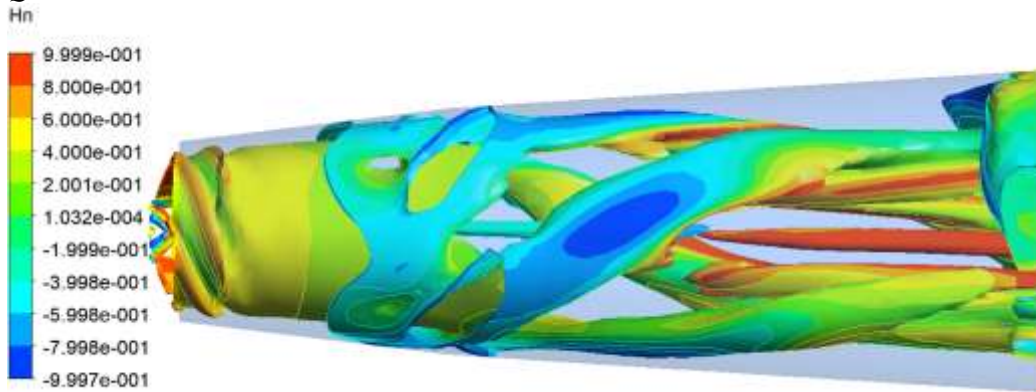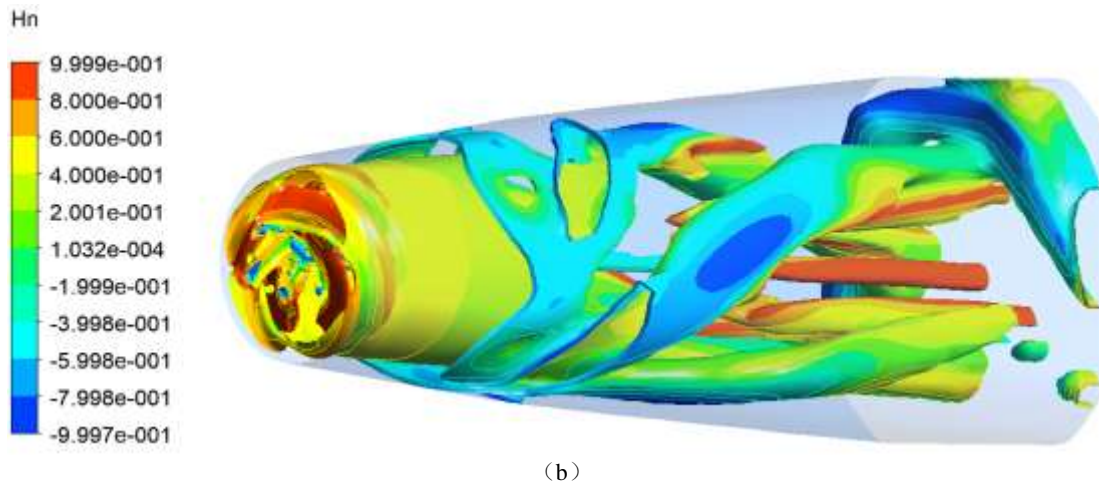
Figure 10: Q=0.230789 s^{-2}

Fig.10 shows the vortex structure in the draft tube of Q=0.230789 s^{-2}. From (a) it can be seen that the vortex distribution near the wall is consistent with the direction of rotation and the previously regularized helicity section.That is to say the direction of swirling of the wall and the center is opposite.It is known from (b) that the direction of swirling of the center is the same as the direction of rotation of the wheel.In terms of rotational strength,the strength of the joint between the draft tube and the runner is very high.As the flow of water flows, the vortex strength at the outlet of the draft tube decreases.In other words,the joint is the main part of noise and pressure pulsation, which is important.The reason is that the vortex intensity is large.
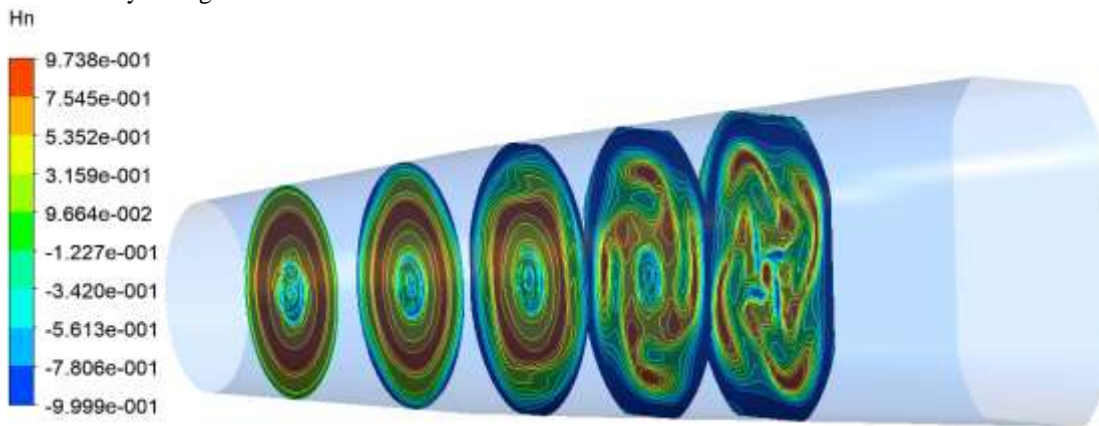
Figure 11: Draft tube section regularized helicity
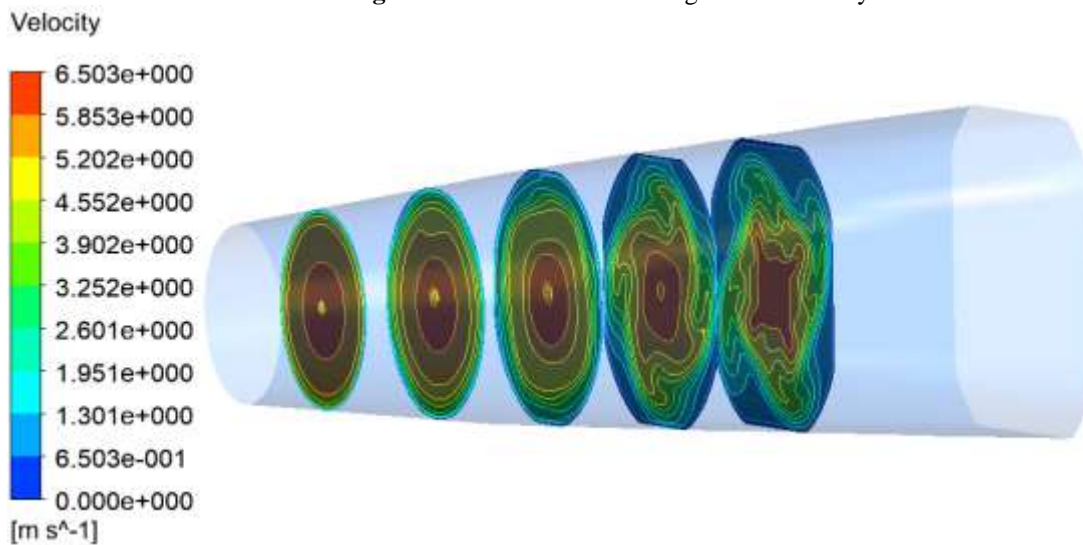
Figure 12: Draft tube section velocity distribution

Fig.11 is a section of the regularized helicity of the five equidistant draft tubes under the Q equivalence plane.It can be seen that the surface vortex distribution near the exit is very obvious,consistent with the previously observed vortex

description near the wall and the center distribution.The velocity distribution in Fig.12 shows only the size distribution of the fluid velocity,and the motion distribution and intensity of the internal vortex are not observed at all.This also proves the feasibility and accuracy of using the vortex dynamics criterion to judge the internal vortex motion of the turbine.

3.3 Runner blade flow diagnosis

From the above analysis,it is known that the surface of the runner blade has a region in which the direction of swirl rotation is opposite.This vortex is highly susceptible to flow separation.In the vortex dynamics,the boundary vorticity is the core concept,which reflects the generation rate of the boundary vorticity,which is the vortex flux entering the fluid through the unit area per unit time.This concept was proposed by Lighthill in 1963 and is defined as:

$$\sigma = v\frac{\partial \omega}{\partial n} \qquad (10)$$

Where v is the coefficient of motion viscosity.n is the unit vector of the normal direction outside the surface of the fluid. ω is the vorticity. σ is the boundary vorticity flow.Boundary vorticity flow is the cause of vorticity field and flow separation[17].It is mainly composed of the following four parts: σ_a generated by wall acceleration. σ_F generated by volume force. σ_π generated by wall normal stress. σ_τ generated by wall tangential stress.For a turbine, the runner is a rotating,non-slip wall,the volumetric force is usually negligible, and the internal flow is at a large Reynolds number,so σ_π is much larger than σ_τ.Therefore,it is only necessary to consider the boundary vorticity generated by the normal stress.For a turbine,the normal stress is actually the pressure.

The axial moment generated by the pressure gradient on the blade surface can be expressed as:

$$M_z = -\int_S (r \times pn)_z \,\mathrm{d}S = -\frac{1}{2}\int_S \rho(r \cdot r)\sigma_{pz}\,\mathrm{d}S + \frac{1}{2}\int_{\partial S} p(r \cdot r)\,\mathrm{d}z \qquad (11)$$

Where M_z is the torque on the rotor blade.S is the surface area of the blade. ∂S is the boundary of the blade surface. σ_{pz} is the Z-axis component of σ_p ,which is the component of the axial direction of the runner,that is the boundary vorticity flow.

It can be seen from the above formula that the area of the first component σ_{pz} on the right side of the formula is on the blade,and the second term on the right is the line integral of the compression moment on the boundary. Therefore,the boundary vorticity flow only considers σ_{pz}.

which is：

$$\sigma = \sigma_\pi = \sigma_p = \frac{1}{\rho}n \times \nabla P = \begin{vmatrix} x & y & z \\ i & j & k \\ \frac{\partial p}{\partial x} & \frac{\partial p}{\partial y} & \frac{\partial p}{\partial z} \end{vmatrix} \qquad (12)$$

$$\sigma_{pz} = \frac{1}{\rho}\left(\frac{\partial p}{\partial y}i - \frac{\partial p}{\partial x}j\right) \qquad (13)$$

The above formula establishes the relationship between the work of the runner and the BVF of the runner blade.Therefore,the blade surface can be diagnosed by the definition of the above formula,and the negative value region of the work can be found from the BVF distribution.

Fig.13 is a distribution diagram of the diagnosis of the rotor blade with BVF.It can be seen from the way that the BVF distribution is very uniform under this condition,which means that the fluid has less negative contribution to the runner under this condition.However,a small amount of peak area can be seen from the enlarged part,the water inlet side of the blade,and the four leaves have the same part.Therefore,it can be judged that the flow of the part is unstable,and the smoothness of the model at the inlet side may be lacking. The diagnosis can be used as a reference. It is necessary to change the geometry of the inlet edge and change the peak area to provide a basis for optimizing the rotor model.It also shows that the BVF diagnostic method is also applicable to the tubular turbine.
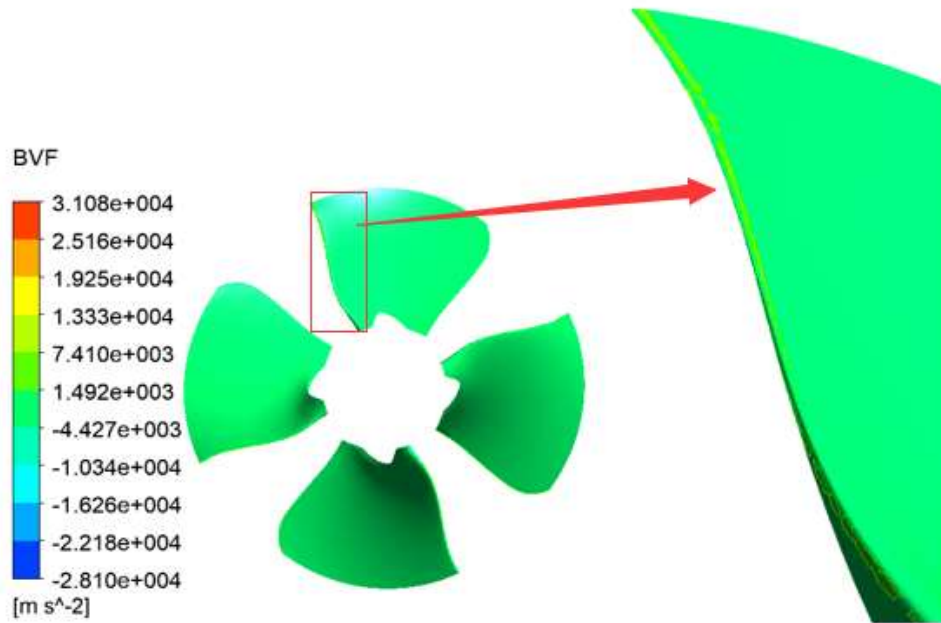
Figure 13: BVF distribution and enlarged part of runner blade surface

According to the theory of vortex dynamics[18],the flow separation criterion is:the surface friction line is concentrated,the BVF line is oriented substantially along the surface friction line,and the BVF has a peak.Separation criterion: the vorticity line has a large curvature.This criterion can determine the occurrence of flow separation at this location,which is a site that needs to be optimized.The mathematical expression is:

$$\frac{\sigma_{\pi}\times\tau}{|\sigma_{\pi}||\tau|}=O\left(\mathrm{Re}^{-1/8}\right) \qquad (14)$$

$$\tau = \mu\omega\times n \qquad (15)$$

It can be seen from Equation (14) that the smaller the Reynolds number, the larger the angle between the BVF line and the friction line.
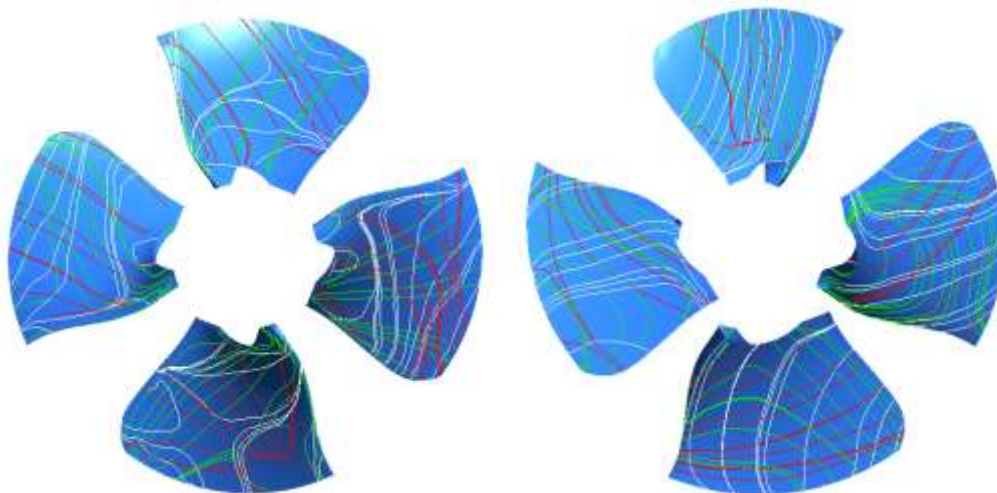
Figure 14: Distribution of BVF lines, friction lines and vorticity lines on the front and back of the runner blades
（Green is the BVF line, red is the friction line, and white is the vorticity line.）

The distribution of the three lines of the front and back of the blade can be clearly seen from Fig.14.First,the red friction line has convergence at the front of the blade near the rim,and the curvature of the vorticity line is larger than the curvature of other regions,so the flow separation can be determined according to the vortex dynamics description.The friction line on the back of the blade is close.Convergence occurred at the hub,and the BVF line was folded along the friction line,indicating that flow separation occurred at the back.It is indicated that the vortex dynamics diagnosis method can accurately determine the flow separation area on the surface of the turbine runner blade, and these areas are the parts that need to be optimized and improved.

4. Test verification

The main design parameters of the hydropower station turbine are:turbine diameter D1=7.2 m,synchronous speed 68.18 r/min, rated output 24.65 MW,rated flow 399.2 m^3/s,maximum head 10 m,rated head 6.8 m,weighted The water head is 7.68 m,the lowest head is 3.1 m,the suction height is allowed to be -8.8 m,and the installation elevation is 1532.2 m.

Table 2: Main technical parameters of bulb tubular turbine

Parameter	Value
Type of Tubular Turbine	GZ995-WP-720
Runner Diameter	7.2 m
Synchronous Speed	68.18 r/min
Rated Output	24.65 MW
Limited Rate	399.2 m^3/s
Maximum Head	10 m
Minimum Head	3.1 m
Rated Head	6.8 m
Weighted Head	7.68 m
Number of Vlades	4
Number of Guide Vanes	16
Allowable Suction Height	-8.8 m
Installation Elevation	1532.2 m

The test was carried out at a hydropower station, and the prototype of the prototype bulb tubular turbine was tested. The test flow range was 295151 kg/m^3 to 340587 kg/m^3, the test head was 8 m,and the uncertainty of the efficiency measurement was ±0.25%.The test method is the exponential method relative efficiency test.By measuring the pressure difference of the flow channel,the exponential flow rate is calculated to replace the real flow.The other main parameters are automatically collected and processed by the "Hydraulic Unit Efficiency Test System",and the relative efficiency and output of the turbine are finally calculated. The test strategy of this real machine test is to carry out the guide vane opening degree of 59.9 °and the blade opening degree of 31 °determined in the process of calculating the association relationship, which not only reduces unnecessary test conditions,but also can be combined with computational simulation results.The comparison is very convenient for the test analysis.

Figure.15 shows the flow rate and efficiency measured at 0.7Q$_d$, 0.8Q$_d$, 0.9Q$_d$, 1.0Q$_d$, 1.1Q$_d$ and 1.2Q$_d$ under six conditions and the pressure curve at a point near the blade.It can be seen from Fig.3 that the numerical values of the efficiency of the six working conditions are higher than the experimental values, and the errors are: 4.39%, 5.21%, 3.79%, 3.56%, 6.28%, and 5.82%, respectively.The computation is more efficient.The measured pressure is slightly larger than the computational simulation,because the computation medium is fresh water,and the actual medium has other mediums causing a large pressure. Because the pressure base is large, it can be seen from the figure that the test is almost identical to the calculated curve. As can be seen from the image, the highest efficiency point flow is also roughly equivalent, and the computation result is basically accurate.
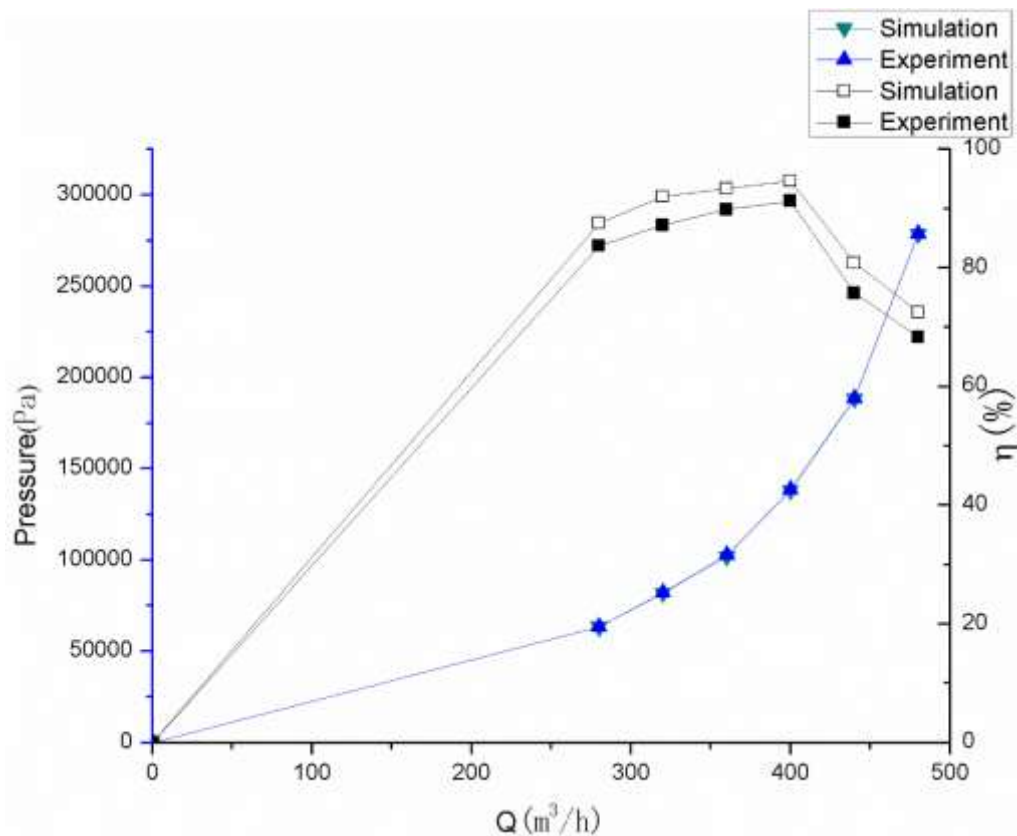
Figure 15:Numerical computation and experimental comparison curve

5. Conclusions

(1) The vortex dynamics regularized helicity criterion is used to observe the internal vortex change of the turbine runner.It is found that there is a vortex with the same direction of rotation and the flow direction of the water flow at the water inlet edge and the hub near the water outlet edge of the turbine runner.At the back of the hub,there is a vortex with a direction of rotation and a direction of flow opposite the inlet.

(2) Applying the *Q*-criterion combined with the regularized helicity in the draft tube,it can be seen that the surface vortex distribution near the exit is very obvious.It is observed that the distribution of the vortex near the wall and the center is consistent,which proves the feasibility and accuracy of using the vortex dynamics criterion to judge the internal vortex motion of the turbine.

(3) The application of vortex dynamics diagnosis found that the flow separation zone and the BVF peak zone on the turbine runner blades capture and amplify the sources of bad flow,which is more accurate than traditional analysis methods. It not only shows that the vortex dynamics diagnosis method is equally effective in the analysis and application of hydraulic turbines,but also provides a new method and idea for the optimization of turbine blades of tubular turbines in the future.

References

[1] Cheng Liangjun. Hydraulic Turbine.*Beijing:China Machine Press*,1981.
[2] Li Fengchao,Fan Honggang,Wang Zhengwei,et al.Optimum design of runner blades of a tubular turbine based on vorticity dynamics[J].*Journal of Tsinghua University（Science and Technology）*,2011,51(06):836-839.
[3] Tong Binggang,Yin Xieyuan,Zhu Keqin. Vorticity dynamic theory[M].Hefei: China University of Science and Technology Press,2009.

[4] Zhang Hanxin. Structural Analysis of Separation Flow and Vortex Motion[M].*Beijing: National Defense Industry Press*,2002.

[5] Jiang M,Machiraju R,Thompson D. Detection and Visualization of Vortices[J]. *Visualization Handbook*,2005:295-309.

[6] Wu Xiaojing,Wu Yulin,et al. Vorticity analysis of a Francis turbine runner[J]. *Journal of Hydroelectric Engineering*, 2008(03):132-136+131.

[7] Zhang Liang,Liu Shuhong,et al. Vorticity dynamics analysis of flow field in Francis runner[J]. *Journal of Hydroelectric Engineering*, 2007(06):106-110.

[8] Yang Lin,Fan Honggang,Chen Naixiang. Bidirectional flow diagnosis to optimize the design of a pump-turbine runner using vorticity dynamics theory[J]. *Journal of Tsinghua University（Science and Technology)*,2007(05):686-690.

[9] Fan Honggang,Chen Naixiang,Yang Lin. Three dimensional flow diagnosis of the pump turbine runner based on the dynamic vorticity[J]. *Journal of Hydroelectric Engineering*, 2007,26(3) :124-128.

[10] Zhao Binjuan,Zhao Youfei,et al. Boundary Vorticity Flux Analysis and Hydraulic Optimization of Double-channel Pump Impeller[J]. *Transactions of the Chinese Society for Agricultural Machinery*,2016,47(10):85-90.

[11] Zhao Youfei.Study on Hydraulic Optimization of the Centrifigal Pump's Impeller Based on Theories of Boundary Vorticity Dynamics[D].*Jiangsu University*,2017.

[12] Wang Yang,Zhao Lifeng,et al. Numerical prediction of multistage centrifugal pump performance and analysis of vorticity of flow field[J].*Journal of Drainage and Irrigation Machinery Engineering*,2016,34(07):561-566.

[13] Zhang Desheng,Zhang Qihua,Shi Weidong.Basic Theory and Application of Pump Design CFD Simulation[M].*Beijing: China Machine Press*,2015.

[14] Hu Zijun, Zhang Lan, Yao Huizhi, et al.Vortex identification in the analysis on the topology structure of vortical flow in cavity[J]. *Journal of Ship Mechanics*, 2012(8):839-846.

[15] Y. Levy, D. Degani, and A. Seginer. Graphical Visualization of Vortical Flows by Means of Helicity[J]. *AIAA J.*,1990(28), 8:1347-1352.

[16] Wang Weijun, Wang Yang, Liu Ruihua. Numerical calculation of cavitation flow in a centrifugal pump[J].*Transactions of the Chinese Society for Agricultural Machinery*, 2014, 45(3):37-44.

[17] Jin-ya Zhang , Shu-jie Cai, Yong-jiang Li, etal. Optimization design of multiphase pump impeller based on combined genetic algorithm and boundary vortex flux diagnosis. 2017,29(6):1023-1034.

[18] WU Jiezh i, MA Huiyang , ZHOU Mingde. In troduction to Vorticity and Vortex Dynamics [M]. *Beijing: Higher Education Press*, 1993.

[19]Cao Puyu, Yin Gang, Wang Yang, et al. Numerical analysis of double tornado-type separation vortices in centrifugal pump[J]. *Transactions of the Chinese Society for Agricultural Machinery*,2016, 47(4):22-28.